Investigation on mode matching including thermal effects in LD end-pumped passively mode-locked Nd:YVO_4 laser

Xiapaketi Wushouer (夏帕克提·吾守尔), Haijuan Yu (于海娟), Ping Yan (闫 平)*, and Mali Gong (巩马理)

Center for Photonics and Electronics, Department of Precision Instruments and Mechanology, Tsinghua University, Beijing 100084, China

**E-mail: pyan@mail.tsinghua.edu.cn*

Received March 18, 2010

We design a laser diode (LD) end-pumped passively mode-locked solid-state laser with a semiconductor saturable absorber mirror. Mode-matching efficiency in the active medium including the thermal effect is analyzed, and the optimum mode-matching coefficient is obtained by optimizing the pump mode. In the experiment, a total power of 4.2 W stable pulse sequences without multipulse at 1064 nm is obtained with a pulse repetition rate of 86 MHz and a pulse width of 13 ps, corresponding to a high optical to optical efficiency of 44%.

OCIS codes: 140.4050, 140.7090, 140.3538.
doi: 10.3788/COL20100810.1004.

The solid-state and fiber lasers play an important role and are used in many field, such as material processing, sensor, and military applications[1−4]. Along with the development of ultrafast laser technology, pulse sequences with ultra short duration, high repetition rate, and high peak intensity can be generated from mode locking[5]. The diode-pumped passively mode-locked all-solid-state laser has widespread applications in laser display, nonlinear frequency conversion, and high-precision micromachining[6]. On the other hand, the use of end-pumped passively mode-locked solid-state Nd^{3+} lasers with saturable absorber[7] is a promising approach in these fields. The saturable absorber can be optimized independent of the cavity design, enabling successful mode locking with a broad range of solid-state laser tools and cavity designs[8,9]. A semiconductor saturable absorber mirror (SESAM), which is a saturable absorber integrated into a mirror structure, is mostly used as the end mirror of a standing wave laser cavity[10−15]. Nd^{3+} host media, such as Nd:YVO_4 and Nd:YAG, have been widely used in solid-state lasers. Compared with Nd:YAG, Nd:YVO_4 has a larger stimulated emission cross section[16,17], a comparatively shorter upper state lifetime[18], and wider pumping wavelength bandwidth[19], making it extremely suitable for achieving continuous mode-locked operation.

Recently, Jabczyński *et al.* reported that they have achieved an optical to optical efficiency of 35% with a pulse width of 15–20 ps for diode bar-pumped continuous wave (CW) mode-locked Nd:YVO_4 laser[20]. In another study, a 43% efficiency was achieved in passively mode-locked YVO_4/$NdYVO_4$ composite crystal laser with a semiconductor saturable absorber as a high reflector[21]. In addition, the end-pumped configuration provides a high degree of spatial overlap between pump and laser modes, and a fiber-coupled diode enables efficient mode matching between the pump volume and the laser mode[22]. Thus, mode-matching efficiency and thermal lenses are valuable in analyzing gain media Nd:YVO_4 crystal because they affect the efficiency of the output power M^2 factor and the stability of the laser oscillator. Li *et al.*[23] analyzed temperature distribution and thermal lensing in laser medium to design a special cavity that can keep the power density on SESAM under its damage threshold.

In this letter, we discuss the mode matching including the thermal effect in laser diode (LD) end-pumped passively mode-locked Nd:YVO_4 laser with SESAM, corresponding to the optimal pump mode. A stable pulse sequence without multipulse with a total power of 4.2 W and beam quality of $M^2 < 1.14$ is also obtained. An optical to optical efficiency of 44% is achieved for stable CW mode-locking operation at 1064 nm, with a pulse repetition rate of 86 MHz and pulse width of 13 ps.

The experimental setup of the LD end-pumped passively mode-locked solid-state laser with SESAM is shown in Fig. 1.

Pump power at 808 nm came from a highly bright fiber-coupled LD (manufactured by NUFERN), which provided an output power of up to 20 W. The fiber had a core diameter of 400 μm and a numerical aperture (NA) of 0.22. The temperature of the LD was controlled by a temperature control unit to obtain the best absorption. The pump laser at 808 nm was focused onto the crystal by a four-lens coupling system. The a-cut Nd:YVO_4 crystal used in our experiment was wedged and had a Nd^{3+}-doping concentration of 0.3 at.-% and dimension of 3×3×9 (mm). The left side of the Nd:YVO_4 was coated with an antireflective (AR) film at 808 nm; the other side of the crystal was AR-coated at 808 and 1064 nm. To

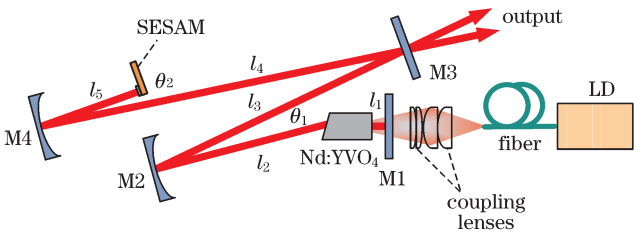

Fig. 1. Experimental setup of a LD end-pumped passively mode-locked solid-state laser with SESAM.

reduce the thermal load, the crystal was wrapped with indium foil and packed inside a copper holder. The LD and crystal were cooled in 15 °C circulating water. M1 is a flat mirror AR-coated at 808 nm and high reflective (HR) coated at 1064 nm, whereas M3 is also a flat mirror used as the output coupler with T=10% at 1064 nm. M2 and M4 are concave mirrors HR-coated at 1064 nm, with radii of curvature of R_1=500 mm and R_2=208 mm, respectively. The included angle between incident and reflected beams on M2 and M4 were θ_1 and θ_2, respectively. The laser crystal Nd:YVO_4 was placed very close to end mirror M1 to enhance spatial hole burning and shorten the pulse width[24].

To achieve a stable CW mode-locking operation, we designated the total cavity length as 1708 mm (l_1+l_2=265 mm, l_3=839 mm, l_4=488 mm, and l_5=116 mm). The SESAM (Batop Gmbh, Germany) was used as the end mirror of the cavity and simply mounted on a small copper heat sink without active cooling. Its absorption ratio and modulation depth were 2% and 1.2%, respectively.

For the theoretical analysis, the experimental setup can be simplified as a model of the end-pumped solid-state laser. Figure 2 shows the schematic of the laser crystal and the definitions of related parameters.

In the model, the two concave mirrors M2 and M4 were replaced by the lenses with foci of $f_{1\mathrm{t}} = \frac{R_1}{2}\cos(\frac{\theta_1}{2})$ and $f_{2\mathrm{t}} = \frac{R_2}{2}\cos(\frac{\theta_2}{2})$ on the meridian plane, and $f_{1\mathrm{s}} = \frac{R_1}{2}/\cos(\frac{\theta_1}{2})$ and $f_{2\mathrm{s}} = \frac{R_2}{2}/\cos(\frac{\theta_2}{2})$ on the sagittal plane. The SESAM used as the end mirror of the laser cavity was replaced by the flat mirror M2′. The far-field half-angle and focal plane position of the pumping beam in the active medium (taking the incidence surface of the crystal as the original point) are θ_p and z_0, respectively, where w_{p0} is the radius of the beam waist and w_{p}(z) is the pumping size along the z-axis.

The intensity distribution of the output beam from a fiber-coupled LD may be described by the circular Gaussian function as[25]

$$P(x,y,z) = P_0 \exp\big[-2\frac{x^2+y^2}{w_{\mathrm{p}}^2(z)} - \alpha z\big], \tag{1}$$

where α is the crystal absorption coefficient for pumping light. The pumping size along the z-axis is given as

$$w_{\mathrm{p}}(z) = \sqrt{w_{\mathrm{p0}}^2 + \theta_{\mathrm{p}}^2(z-z_0)^2}. \tag{2}$$

A more practical distribution of the output beam intensity from the fiber-coupled LD may be closer to a super Gaussian function. In the experiment, we used the 90/10 knife-edge method to measure the transverse intensity distribution of the output pump mode. From the measurement results, a four-order super Gaussian function can be used to precisely describe the transverse intensity distribution of the output pump mode in the beam waist and far field.

Effective mode volume V_{eff} and mode-matching coefficient η_{m} can be defined as[26]

$$V_{\mathrm{eff}} = \big[\iiint s_{\mathrm{l}}(x,y,z) r_{\mathrm{p}}(x,y,z)\mathrm{d}v\big]^{-1}, \tag{3}$$

$$\eta_{\mathrm{m}} = \frac{\big[\iiint s_{\mathrm{l}}(x,y,z) r_{\mathrm{p}}(x,y,z)\mathrm{d}v\big]^2}{\iiint s_{\mathrm{l}}^2(x,y,z) r_{\mathrm{p}}(x,y,z)\mathrm{d}v}, \tag{4}$$

where $s_{\mathrm{l}}(x,y,z)$ is the normalized cavity mode intensity distribution, and $r_{\mathrm{p}}(x,y,z)$ is the normalized pump intensity distribution in the active medium. The mode-matching coefficient varies with pump beam waist radius w_{p0}, and its location z_0 is the distance between the incident face of the crystal and the pump beam waist spot in the crystal. For a single transverse mode TEM_{00}, $s_{\mathrm{l}}(x,y,z)$ can be given by

$$s_{\mathrm{l}}(x,y,z) = \frac{2}{\pi w_{\mathrm{l}}^2(z) l} \exp\big[-2\frac{x^2+y^2}{w_{\mathrm{l}}^2(z)}\big], \tag{5}$$

where $w_{\mathrm{l}}(z)$ is the cavity mode size along the z-axis, and l is the length of the active medium. For a fiber-coupled pump beam, the normalized pump intensity distribution in the active medium is written as

$$r_{\mathrm{p}}(x,y,z) = \frac{\alpha \mathrm{e}^{-\alpha z}}{\pi w_{\mathrm{p}}^2(z)(1-\mathrm{e}^{-\alpha l})} \Theta[w_{\mathrm{p}}^2(z) - x^2 - y^2], \tag{6}$$

where $\Theta(\cdots)$ is the Heaviside step function. The profile of the beam (TEM_{00} mode radius) in the laser resonator is calculated based on the standard $ABCD$ matrix and by considering the thermal lens effect of the laser medium.

The radius of the cavity mode at the surface of the crystal is w_{l}=0.197 mm at a thermal lens length of 100 mm. Based on Eqs. (1)−(6), the numerical result of the mode-matching coefficient in our experimental setup is obtained and shown in Fig. 3.

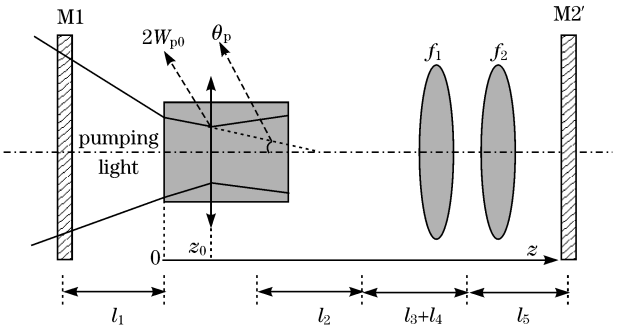

Fig. 2. Schematic of experimental setup.

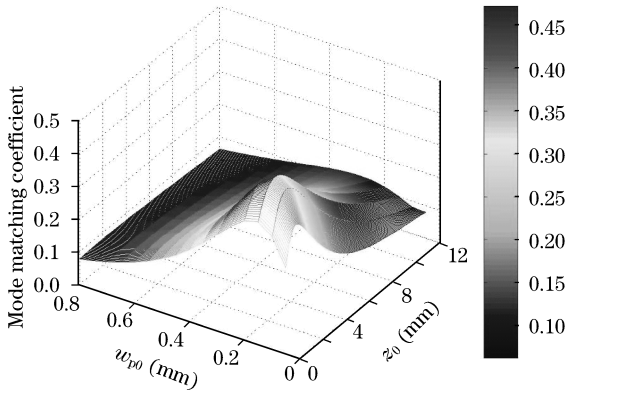

Fig. 3. Mode-matching coefficient varying with pump beam waist radius w_{p0} and its location z_0 in the crystal.

At a pump power of 12 W, the radius optimal pump size of w_{p0}=0.21 mm and the optimal location of pump waist spot of z_0=1.5 mm can be obtained by a numerical computation with the highest mode-matching coefficient of 47.2%.

Thermal effect plays an important role in laser performance[27,28]. For an end-pumped structure with a fiber-coupled LD, taking the intensity attenuation along the z direction into account provides the thermal focal length as follows[29]:

$$\frac{1}{f_T}=\int_l^0 \frac{P_t}{2\pi K_c}\cdot\frac{\alpha e^{-\alpha z}}{1-e^{-\alpha l}}\cdot\frac{[dn/dT+(n-1)\alpha_T]}{\omega_p^2(z)}dz, \tag{7}$$

where f_T is the thermal focal length, K_c denotes the thermo-conductivity, dn/dT is the thermo-optical coefficient, P_t stands for the power translated from the pumping source into the heat load in the laser medium, α_T is the thermal expansion coefficient, and n is the crystal index.

The a-cut Nd:YVO_4 used in our experiment has a Nd^{3+} doping concentration of 0.3 at.-% with dimensions of 3×3×9 (mm). Therefore, the thermal focal length can be calculated using the following parameters: the thermo-conductivity K_c=0.0523 W/(K·cm), the thermo-optical coefficient $dn/dT=3.0\times10^{-6}$ K^{-1}, the pump beam waist in crystal w_{p0}=0.27 mm, the crystal index n_c=2.165, the length of crystal l=9 mm, the crystal absorption coefficient α=6.0 cm^{-1}, and thermal expansion coefficient $\alpha_{Ta}=4.43\times10^{-6}$ K^{-1}. By numerically solving Eq. (7), we obtain the thermal focal length at different levels of pump power, and also acquire mode radii (in the laser crystal and on SESAM) varying with from the experimental pump power. From Fig. 4, it can be also seen that TEM_{00} mode radii in the crystal and on SESAM decrease with the pump power.

For stable CW mode locking, the criterion for a stable mode-locking laser with a SESAM is given by[30]

$$\frac{2LP_{out}}{cT}\geq\pi\sqrt{F_{sat,a}\omega_a^2F_{sat,g}\omega_g^2\Delta R}\,, \tag{8}$$

where L is the length of the cavity, P_{out} is the output power of the laser, c denotes the speed of light in a vacuum, T represents the output coupler transmission, ΔR is the modulation depth of the SESAM, ω_a and ω_g are the values of intensity radius of the laser beam on the SESAM and in the gain medium, respectively. The saturation fluences of the SESAM and the gain medium are $F_{sat,a}$ and $F_{sat,g}$, respectively.

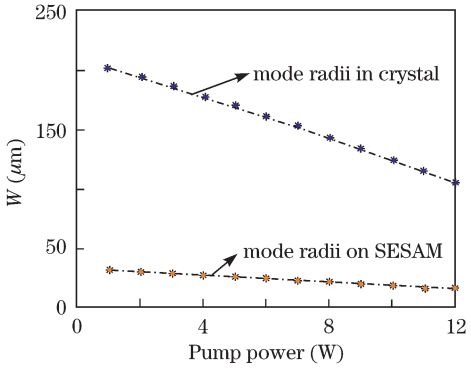

Fig. 4. Radius of cavity mode (in laser crystal and on SESAM) varying with pump power.

To obtain stable CW mode locking, Eq. (8) must be satisfied by increasing the length of the cavity, reducing the transmissivity of the output coupler and decreasing the values of the intensity radius of the laser beam on the SESAM and in the crystal. The intracavity pulse fluence is supposed to be kept three to five times the saturation fluence of the SESAM because obtaining mode locking is difficult if the value of the impulsion fluence is too small. During the experiments, the value of the impulsion fluence was controlled by adjusting the value of the intensity radius of the laser beam on the SESAM (ω_a). The energy of a mode-locked pulse in the cavity is defined as $E_P=2LP_{out}/cT$; thus, the minimum intracavity pulse energy is $E_{P,c}=\pi\sqrt{F_{sat,a}\omega_a^2F_{sat,g}\omega_g^2\Delta R}$. The laser operates in Q-switched mode locking (QML) with $E_P<E_{P,c}$, and the laser operates in CW mode locking with $E_P>E_{P,c}$.

In our experiment, we modified the output coupling to adjust the intracavity power and obtain the stable mode-locked CW operation. The mode size in the crystal and on the SESAM can be adjusted by a telescope

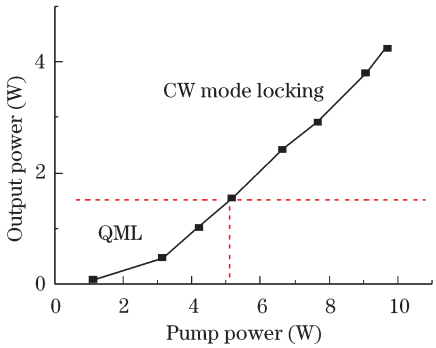

Fig. 5. Output power in Q-switched and CW passively mode-locked regimes.

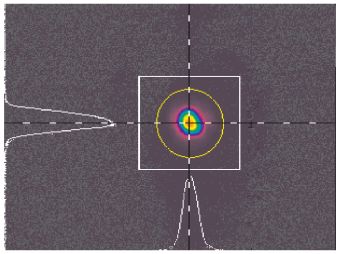

Fig. 6. Spatial form for output laser of a LD end-pumped passively mode-locked solid-state laser with SESAM.

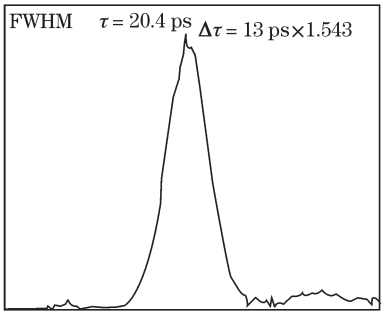

Fig. 7. Measured autocorrelation trace.

optical system consisting of concave mirrors in the cavity, and individually controlled by M2 and M4. The saturation fluences of the SESAM and the gain medium are $F_{\mathrm{sat,a}}$ =70 μJ/cm^2 and $F_{\mathrm{sat,g}}$ =0.12 J/cm^2, respectively. At a pump power of 6 W, the stable CW mode-locked operation is achieved with 42-μm mode radii on the SESAM and 154-μm mode radii in the laser crystal for an output coupling of 10%. Thus, the minimum intracavity pulse energy $E_{\mathrm{P,c}}$ obtained is 0.07 μJ.

Based on the analysis of the mode-matching coefficient, the optimal pump mode can be fixed at w_{p0}=0.2 mm and z_0=1.5 mm by adjusting the four-lens coupling system. From an output power of 0.5 W (pump power of 3 W), the intracavity pulse energy is E_{P}=0.06 μJ (E_{P}<$E_{\mathrm{P,c}}$), and the laser is in stable QML stage. When the output power increases to 2 W (pump power of 6 W), the intracavity pulse energy is E_{P}=0.23 μJ (E_{P}>$E_{\mathrm{P,c}}$), and the CW mode locking appears in the laser cavity.

In a stable CW mode-locking operation, we achieve an average power of 4.22 W at the pump power of 9.5 W, corresponding to an optical to optical efficiency of 44% and a slope efficiency of 56.7%, as shown in Fig. 5. The TEM$_{00}$ beam quality factors are M_x^2=1.08 and M_y^2=1.14, measured with a Spiricon M2-200 laser beam analyzer (Fig. 6).

When the stable mode locking is captured, the repetition of the impulse sequence is 86 MHz, measured by a digital oscilloscope, and the spectrum width of the output beam is 0.16 nm, corresponding to Δv=42.4 GHz. The pulse width was measured using an autocorrelator (APE Company, Germany), and Fig. 7 shows the profile of an autocorrelation signal with a full-width at half-maximum (FWHM) of 20.4 ps in a range of 150 ps. However, in a range of 600 ps, we find that a multipulse is induced by the Fabry-Perot (F-P) effect generated in the laser crystal, which reduces the peak power of the output laser. Therefore, we positioned the laser crystal at an incline or made a wedged type laser crystal to avoid the multipulse. Taking a hyperbolic secant (sech2), we estimated the pulse duration to be $\Delta\tau$=13 ps×1.543. The time-bandwidth product is $\Delta\tau\Delta v$=0.55.

In conclusion, we have demonstrated a LD-pumped passively mode-locked solid-state laser with SESAM, and discussed the mode-matching efficiency in the active medium to obtain the optimal pump mode including the thermal effect. The laser cavity can produce a stable pulse sequence without multipulse with a total power of 4.2 W and good beam quality ($M^2 < 1.14$). The optical to optical efficiency of 44% is achieved for a stable CW mode-locking operation at 1064 nm, with a pulse repetition rate of 86 MHz, a linewidth of 0.16 nm, and a pulse width of 13 ps.

This work was partially supported by the State Key Laboratory of Tribology, Tsinghua University under Grant No. SKLT08A05.

References

1. P. Yan, S. Yin, and M. Gong, Chin. Opt. Lett. **6,** 580 (2008).
2. S. Yin, P. Yan, C. Li, and M. Gong, Chinese J. Lasers (in Chinese) **35,** 835 (2008).
3. B. Peng, Q. Liu, M. Gong, and P. Yan, Chinese J. Lasers (in Chinese) **35,** 343 (2008).
4. H. Liu, Y. Sun, S. Zhang, T. Li, and J. Li, Chin. Opt. Lett. **6,** 361 (2008).
5. U. Keller, K. J. Weingarten, F. X. Kärtner, D. Kopf, B. Braun, I. D. Jung, R. Fluck, C. Hönninger, N. Matuschek, and J. A. der. Au, IEEE J. Sel. Top. Quantum Electron. **2,** 435 (1996).
6. U. Keller, Nature **424,** 831 (2003).
7. C. Gerhard, F. Druon, P. Georges, V. Couderc, and P. Leproux, Opt. Express **14,** 7093 (2006).
8. L. E. Adams, E. S. Kintzer, M. Ramaswamy, J. G. Fujimoto, U. Keller, and M. T. Asom, Opt. Lett. **18,** 1940 (1993).
9. L. R. Brovelli, U. Keller, and T. H. Chiu, J. Opt. Soc. Am. B **12,** 311 (1995).
10. L. Guo, W. Hou, H.-B. Zhang, Z.-P. Sun, D. Cui, Z.-Y. Xu, Y.-G. Wang, and X.-Y. Ma, Opt. Express **13,** 4085 (2005).
11. J.-L. He, Y.-X. Fan, J. Du, Y.-G. Wang, S. Liu, H.-T. Wang, L.-H. Zhang, and Y. Hang, Opt. Lett. **29,** 2803 (2004).
12. A. Agnesi, F. Pirzio, A. Tomaselli, and G. Reali, Opt. Express **13,** 5302 (2005).
13. Y. F. Chen, S. W. Tsai, Y. P. Lan, S. C. Wang, and K. F. Huang, Opt. Lett. **26,** 199 (2001).
14. H. Luo, D. Y. Tang, G. Q. Xie, H. J. Zhang, L. J. Qin, H. H. Yu, L. Y. Ng, and L. J. Qian, Opt. Commun. **281,** 5382 (2008).
15. Z. Cai, P. Wang, W. Wen, X. Ding, and J. Yao, Chinese J. Lasers (in Chinese) **34,** 901 (2007).
16. X. Yan, Q. Lin, X. Fu, H. Chen, M. Gong, and D. Wang, Opt. Express **17,** 21956 (2009).
17. H. Zhang, M. Gao, Y. Zheng, and J. Yao, Chinese J. Lasers (in Chinese) **31,** 19 (2004).
18. L. McDonagh, R. Wallenstein, R. Knappe, and A. Nebel, Opt. Lett. **31,** 3297 (2006).
19. Y. F. Chen, Y. P. Lan, and S. C. Wang, Opt. Lett. **25,** 1016 (2000).
20. J. K. Jabczyński, W. Żendzian, and J. Kwiatkowski, Opto-Electronics Review **14,** 135 (2006).
21. Z. Zhuo, T. Li, and Y.-G. Wang, Laser Phys. Lett. **1,** 1 (2008).
22. X. Yan, Q. Liu, L. Huang, Y. Wang, X. Huang, D. Wang, and M. Gong, Laser Phys. Lett. **5,** 185 (2008).
23. T. Li, S. Zhao, Z. Zhuo, and Y. Wang, Opt. Commun. **282,** 940 (2009).
24. B. Braun, K. J. Weingarten, F. X. Kärtner, and U. Keller, Appl. Phys. B **61,** 429 (1995).
25. M. Gong, C. Lu, P. Yan, and Y. Wang, IEEE J. Quantum Electron. **44,** 1009 (2008).
26. Y. F. Chen, T. M. Huang, C. F. Kao, C. L. Wang, and S. C. Wang, IEEE J. Quantum Electron. **33,** 1424 (1997).
27. Z. Xiong, Z. G. Li, N. Moore, W. L. Huang, and G. C. Lim, IEEE J. Quantum Electron. **39,** 979 (2003).
28. W. Xie, S.-C. Tam, Y.-L. Lam, J. Liu, H. Yang, J. Gu, and W. Tan, Appl. Opt. **39,** 5482 (2000).
29. M. E. Innocenzi, H. T. Yura, C. L. Fincher, and R. A. Fields, Appl. Phys. Lett. **56,** 1831 (1990).
30. C. Hönninger, R. Paschotta, F. Morier-Genoud, M. Moser, and U. Keller, J. Opt. Soc. Am. B **16,** 46 (1999).